www.czasopisma.pan.pl PAN POLSKA AKADEMIA NAUK www.journals.pan.pl

A R C H I V E S O F M E T A L L U R G Y A N D M A T E R I A L S

Volume 60 2015 Issue 2

DOI: 10.1515/amm-2015-0114

JIN MAN JANG*, WONSIK LEE*,♯, SE-HYUN KO*, CHULWOONG HAN*, HANSHIN CHOI*

OXIDE FORMATION IN METAL INJECTION MOLDING OF 316L STAINLESS STEEL

TWORZENIE TLENKÓW PODCZAS WTRYSKIWANIA PROSZKU STALI NIERDZEWNEJ 316L

The effects of sintering condition and powder size on the microstructure of MIMed parts were investigated using water-atomized 316L stainless steel powder. The 316L stainless steel feedstock was injected into micro mold with micro features of various shapes and dimensions. The green parts were debound and pre-sintered at 800°C in hydrogen atmosphere and then sintered at 1300°C and 1350°C in argon atmosphere of 5torr and 760torr, respectively. The oxide particles were formed and distributed homogeneously inside the sample except for the outermost region regardless of sintering condition and powder size. The width of layer without oxide particles are increased with decrease of sintering atmosphere pressure and powder size. The fine oxides act as the obstacle on grain growth and the high sintering temperature causes severe grain growth in micro features due to larger amount of heat gain than that in macro ones.

Keywords: Powder injection molding, Sintering, 316L stainless steel, Sintering atmosphere, Micro part

1. Introduction

In the last decade, demand of miniaturization has been enlarged in several industrial fields such as electronics, healthcare, automobiles and environmental monitoring, etc [1, 2]. Especially, significance of metallic and ceramic micro parts seems being increased largely for application to chemical and dynamic systems, owing to their excellent corrosion resistant, magnetic and mechanical properties. These micro components can be manufactured by several micro mechanical technologies such as micro powder injection molding (μ-PIM), rapid prototyping (RP), micro-electroforming, micromachining and micro-forging etc. Among them, μ-PIM offers significant advantages in productivity and mass production and thus, is one of the most possible processes for miniaturization [3-6].

Micro PIM has the same four main steps as typical PIM; mixing, injection molding, debinding and sintering. Feedstock, produced by mixing powder and polymeric binder, is used as a material in PIM. The feedstock is injected into the mold cavity and then the binder in the green part is removed by various debinding process. The debound part is very brittle and needs to be sintered carefully to achieve its final sintered density and the desired mechanical and dimensional properties. The dimensional properties of micro PIMed parts depend mainly on the sintering conditions because the micro part experiences the large shrinkage during sintering [7-9]. However, it is difficult to control the sintering process because of the relatively large number of influencing parameters. In present work, the effects of sintering condition on the microstructure of micro MIMed parts were investigated using water-atomized 316L stainless steel powder.

2. Experimental

The feedstock for micro MIM was provided from Dai-Ichi Ceramo Co., Ltd, Japan. It was a mixture of polymer binder, wax and 316L type of stainless steel powder. The 316L stainless steel powder used in this work were made by water-atomization and had a mean particle size (D_{50}) of 4μm and 8μm, respectively. The chemical composition of the 316L stainless steel powder is given in Table 1. The 4μm- and 8μm-sized 316L powders were mixed with binder of 41% and 39% in volume fraction, respectively.

TABLE 1
Composition of as-received 316L stainless steel powder (wt. %)

Cr	Ni	Mo	Mn	Si	C	O	Fe
16~18	12~15	2~3	2 max	1 max	0.03max	0.005	Remainder

Injection temperature (barrel temperature) was set to 180°C, based on thermal analysis (SDT Q600, TA Instrument) results of feedstock (Fig. 1), and injection molding was performed at pressure of 3 MPa. A mold was used with various micro features which had different widths and heights in two-dimensional shape, as shown in Fig. 2. After injection, green parts were debound and sintered. For debinding, the green parts were heated to 600°C at heating rate of 0.5°C/min

* KOREA INSTITUTE OF INDUSTRIAL TECHNOLOGY, INCHEON, 406-840, KOREA
♯ Corresponding author: wonslee@kitech.re.kr

under 760torr hydrogen atmosphere and pre-sintered at 800°C to impart handling strength. The debound brown parts were sintered for 3hrs at 1300°C and 1350°C, respectively. Two types of sintering atmosphere control program were performed as follows. The first program was to heat up to sintering temperatures heating in a continuous flow of 760torr argon gas (hereafter, simply referred to as 760torr Ar), the second to heat to 1050°C in a vacuum and up to sintering temperatures in a continuous flow of 5torr argon gas (referred to as 5torr Ar).

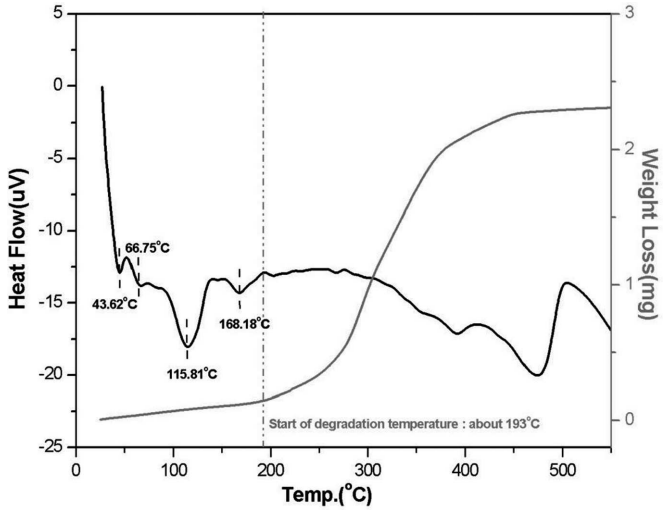

Fig. 1. DTA/TGA results of 316L feedstock used in this study

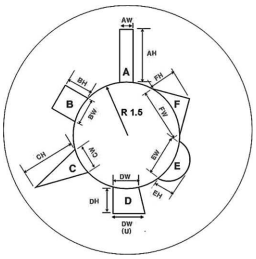

Micro feature	A		B		C	
	AW	AH	BW	BH	CW	CH
Dimension (μm)	250	1000	500	500	500	1000

Micro feature	D			E		F	
	DW	DH	DW(U)	EW	EH	FW	FH
Dimension (μm)	400	500	600	800	400	1000	500

Fig. 2. Schematic drawing of mold cavity and dimension of micro features

After debinding and sintering, the changes of shape and dimension were investigated by a precision measuring microscope (MF-A1010H, Mitutoyo). To investigate the effects of sintering condition and powder size on microstructure of the sintered parts, scanning electron microscopy (QUANTA 200FEG, FEI Company) with EDX (energy-dispersive X-ray spectroscopy) was used.

3. Results

Fig. 3 shows SEM morphologies of debound and sintered parts using 4μm powder feedstock. The micro part pre-sintered at 800°C (Fig. 3(a)) shows sound shape, indicating that the micro features were completely filled into sharp edges with feedstock during injection molding and debound successfully maintaining well shape retention. As can be seen in Fig. 3(b), neither distortion nor cracks in the micro features was observed in the micro part sintered at 1300°C. In the sample sintered at 1350°C, however, micro features have relatively rounded edges compared with sharp edges of the sample sintered at 1300°C.

To investigate the microstructure of the sintered micro parts, the samples were mounted and plane polished. Fig. 4 shows the representative microstructure and EDX results (including mapping results) of the micro part sintered at 1350°C in 760torr Ar atmosphere using 4μm powder feedstock. As shown in Fig. 4, the particles with higher contents of silicon, chrome and oxygen than raw powder were formed and distributed homogeneously inside the sample except for area near surface (the outermost area marked by double-headed arrow).

Fig. 5 shows the changes of the width of particle-free outermost layer and the distribution of oxide particles with powder size and sintering condition (such as temperature and atmosphere). As can be seen in Fig. 5, the outermost layer expands as the sintering atmosphere pressure decreases from 760 torr to 5 torr and the powder size decreases from 8 μm to 4 μm. However, the increase of sintering temperature from 1300°C to 1350°C does not influence largely the increase of the width of outermost layer. Meanwhile, the size of oxide particles is increased with increase of powder size irrespective of sintering conditions. The representative (etched) microstructures in outermost and center regions of sintered micro part are shown in Fig. 6. In the outermost layer without oxide particles, significant grain growth occurred as compared to the region where the particles were homogeneously distributed. Grain size was investigated by EBSD. From the results, the average grain size in the center region with oxide particles was measured to be about 56 um, whereas the grains grew above 150 um at the outermost layer where the small amount of oxides exists.

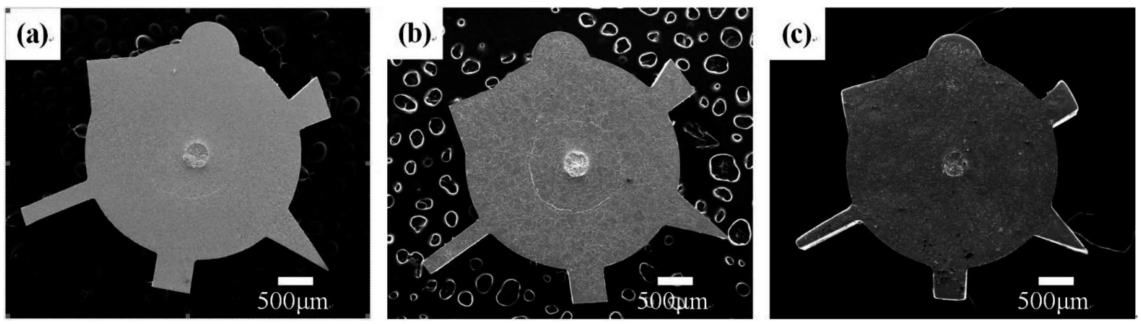

Fig. 3. SEM micrographs of debound and sintered parts using 4 μm powder feedstock : (a) a part pre-sintered at 800°C in 760 torr H_2 atmosphere, (b) a part sintered at 1300°C in 760 torr Ar atmosphere, (c) a part sintered at 1350°C in 5 torr Ar atmosphere

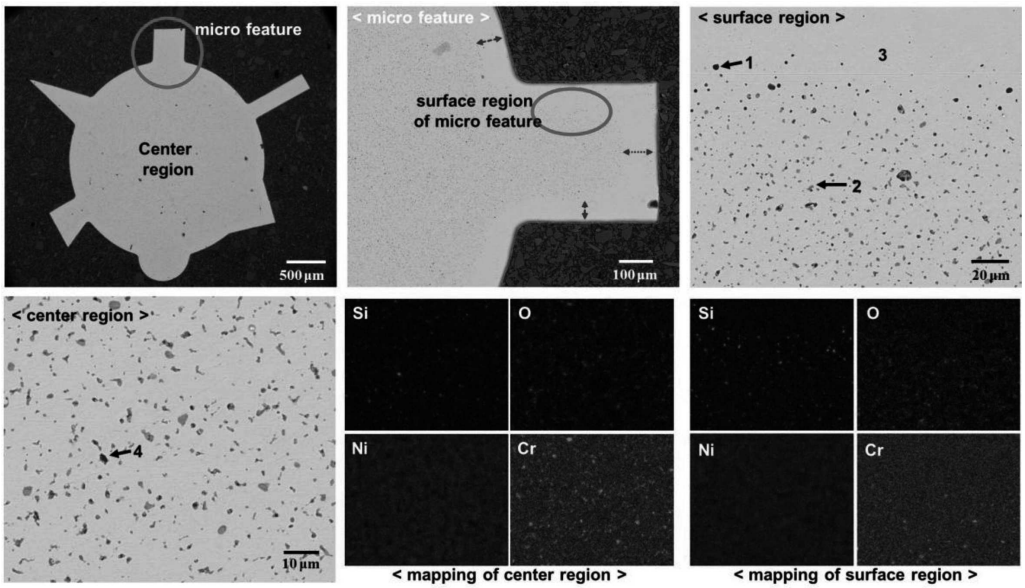

Area	Fe (wt. %)	Cr (wt. %)	Ni (wt. %)	Si (wt. %)	O (wt. %)
1	46.04	14.08	6.67	29.53	3.68
2	51.66	14.95	8.13	22.17	3.09
3	70.05	16.20	13.75	-	-
4	51.81	21.66	8.60	11.78	6.16

Fig. 4. SEM micrographs and EDX results(including mapping results) of the micro part sintered at 1350°C in 760 torr Ar atmosphere using 4 μm powder feedstock

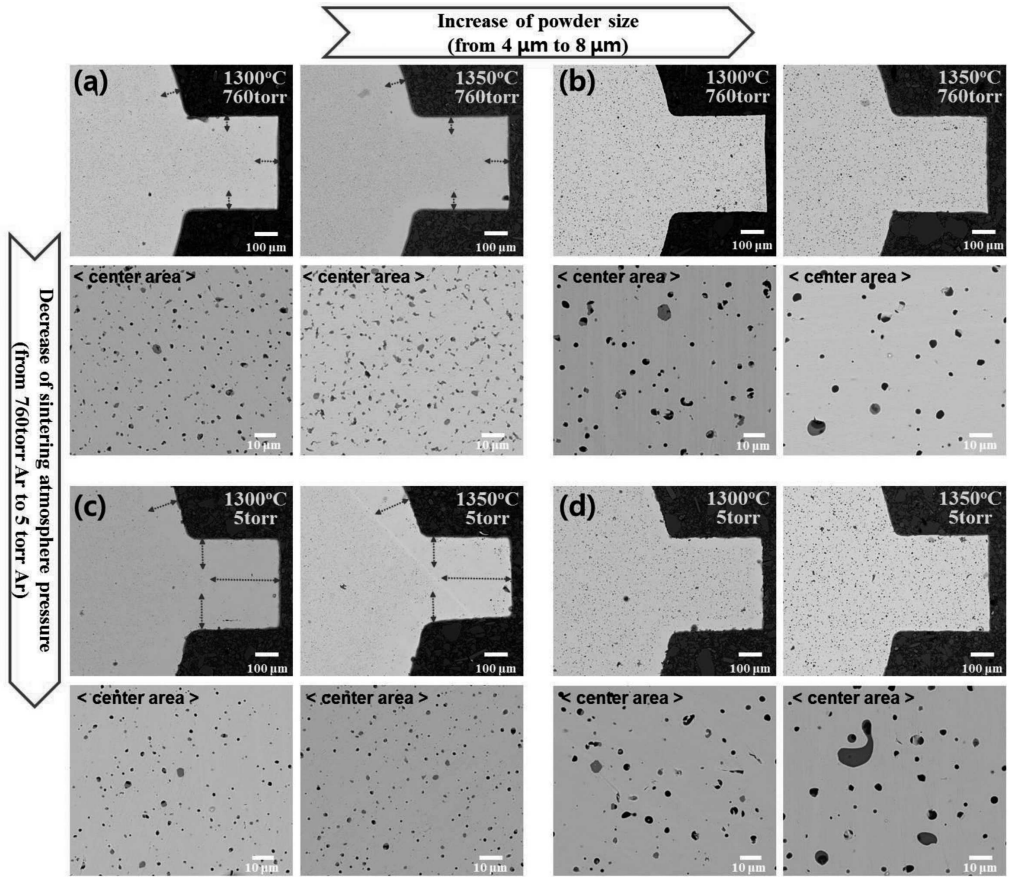

Fig. 5. SEM images of representative micro structures of the samples sintered at different conditions : (a) and (c) are the parts sintered in 760 torr and 5 torr Ar, respectively using 4 μm powder feedstock, and (b) and (d) are those using 8 μm powder feedstock. Double-headed arrow means the width of oxide-free layer

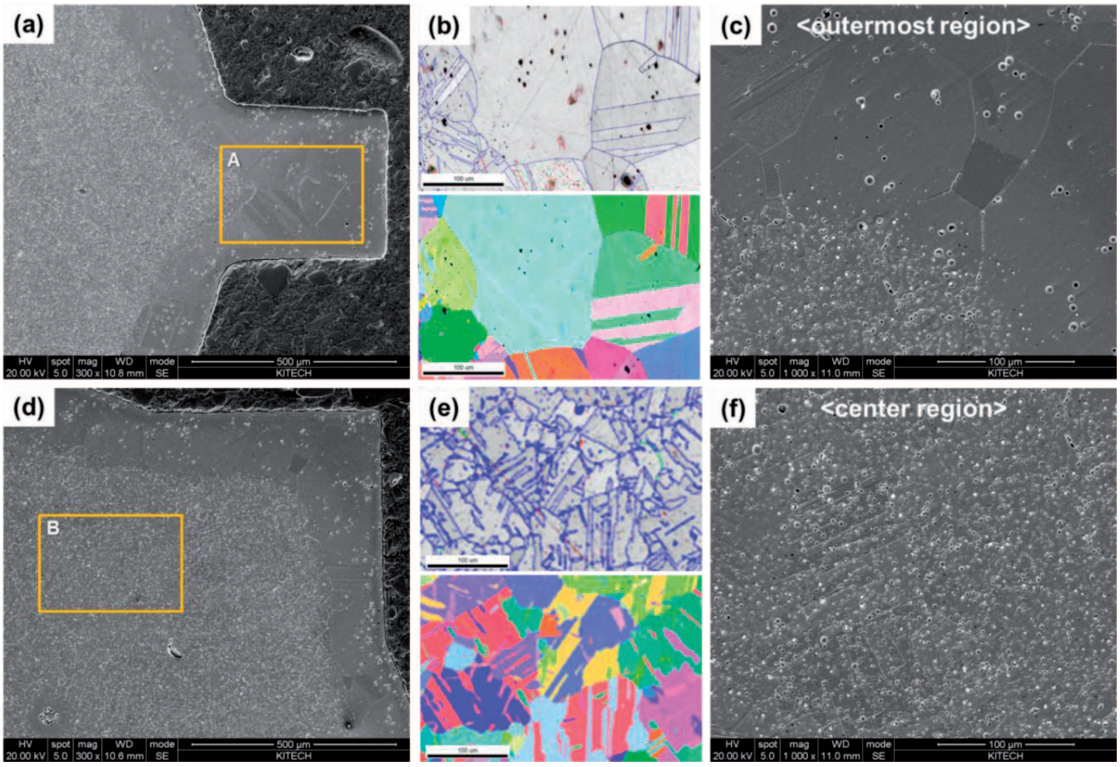

Fig. 6. Microstructures of representative micro feature sintered at 1350^{o}C for 3hrs in 5 torr Ar atmosphere using 4um powder feedstock. (a), (b) and (c) are SEM and EBSD images at the outermost layer and (d), (e) and (f) are those in the center region

4. Discussion

Water atomization leads to oxidation of the powder surface. Thus, the oxide layers including Al, Si, Cr and Fe oxides are formed on the powder surface. The silicon oxide among these oxides becomes discontinuous above 1250°C, and that it is thermodynamically feasible to reduce SiO2 above 1290°C in atmosphere typical in laboratories and practice, and the other oxides are reduced between 1000 and 1200°C [10, 11]. The reduction reaction during sintering in partial pressure of Ar atmosphere is occurred by reaction of residual carbon and oxide, resulting in CO gaseous product. The residual carbon is due to incomplete debinding and it is known generally that small amount of binder always remains after debinding process.

Fig. 5 indicates that the outermost layer without the oxides broadens with decrease of the atmosphere pressure and powder size. This can be explained by pore closure and pressure difference between sintering atmosphere and sample inside. As the sintering temperature increases, the pressure of CO gas of reduction product increases within sample, resulting in pressure difference between sintering atmosphere and sample inside. Due to the pressure difference, CO gas diffuses out from sample inside and the diffusivity increases with decrease of sintering atmosphere pressure, i.e. from 760torr to 5torr. However, according to progress of sintering process, open pores are gradually closed. Thus, the diffusion of CO gas from the inside of sample to the outside becomes difficult and the gas is finally confined in closed pores on the inside of sample, resulting in re-oxidation with metallic elements such as silicon, chromium and iron during cooling. However, in outermost region of sample, the diffusion out of the CO gas can proceeds sufficiently due to shorter transport path during the closure of pores and after sintering, the oxide-free layer in microstructure is formed. In powder size, it is well known that the thickness of oxide layers formed during water atomization process increases with particle size [11, 12]. Hence, the 8μm 316L powder has larger amount of oxide and during sintering, the reduction of the oxides might be incomplete due to insufficient residual carbon or sintering time, comparing to 4μm powder. Also, large pores in the 8μm powders lower the pressure of CO gas within sample and the resultant diffusivity of the gas decreases due to low pressure difference. The inadequate reduction and the low diffusivity leaves large amount of oxide overall sample regardless of the inside or the outside after sintering. Consequently, the larger pressure difference between sintering atmosphere and sample inside and the smaller powder size is the easier the removal of oxide during sintering. Thus, in this study, the widest oxide-free region was obtained in sintering condition of 5torr Ar using 4μm powder feedstock.

The grain growth, being shown in Fig. 6(a), results from the absence of the oxides and high sintering temperature. The fine oxides act as the obstacle on grain growth and the sintering temperature as high as 1350°C causes severe grain growth in micro features due to larger amount of heat gain than that in macro ones.

5. Conclusions

In this work, the effects of sintering condition and powder size on the microstructure of micro MIMed parts were investigated using water-atomized 316L stainless steel powder. The 316L stainless steel feedstock was injected into micro mold. The green parts were debound and pre-sintered at 800°C in

hydrogen atmosphere and then sintered at 1300°C and 1350°C in argon atmosphere of 5torr and 760torr, respectively.

1. The reduction reaction during sintering in partial pressure of Ar atmosphere is occurred by reaction of residual carbon and oxide, resulting in CO gaseous product.
2. The oxide particles are generated by re-oxidation reaction of metallic elements and CO gas confined in pores being closed according to progress of sintering process during cooling, whereas the oxide-free layer in outermost region of the sintered sample is formed by sufficient diffusion out of CO gas due to shorter transport path during closure of pores.
3. The larger pressure difference between sintering atmosphere and sample inside and the smaller powder size is the easier the removal of oxide. Thus, in this study, the widest oxide-free region was obtained in sintering condition of 5torr Ar using 4μm powder feedstock.
4. The fine oxides act as the obstacle on grain growth and the high sintering temperature causes severe grain growth in micro features due to larger amount of heat gain than that in macro ones.

Acknowledgements

We would like to acknowledge the financial support from the R&D Convergence Program of MSIP (Ministry of Science, ICT and Future Planning) and ISTK (Korea Research Council for Industrial Science and Technology) of Republic of Korea (Grant B551179-12-02-00).

REFERENCES

[1] B.Y. Tay, L. Liu, N.H. Loh, S.B. Tor, Y. Murakoshi and R. Maeda, Mater. Char. **57**, 80 (2006).
[2] V. Piotter, W. Bauer, T. Benzler, A. Emde, Microsyst. Tech. **7(3)**, 99 (2001).
[3] Z.Y. Liu, N.H. Loh, S.B. Tor, K.A. Khor, Y. Murakoshi, R. Maeda, T. Shimizu, J. Mater. Process Tech. **127(2)**, 165 (2002).
[4] T. Gietzelt, O. Jacobi, V. Piotter, R. Rupecht, J. Hausselt, J. Mater. Sci. **39(6)**, 2113 (2004).
[5] L. Liu, N.H. Loh, S.B. Tor, K.A. Khor, Y. Murakoshi, R. Maeda, Appl. Phys. A **83**, 31 (2006).
[6] S. W. Kim, J. H. Yang, S. S. Park, Y. D. Kim, I-H. Moon, J. Kor. Powd. Met. Inst. **19(2)**, 117 (2002).
[7] T. J. Garino, A.M. Morales, B.L. Boyce, Microsyst. Tech. **10(6-7)**, 506 (2004).
[8] T. Beck, J. Schneider, V. Schulze, Microsyst. Tech. **10(3)**, 227 (2004).
[9] B-H. Cha, J-S. Lee, J. Kor. Powd. Met. Inst. **16(5)**, 342 (2009).
[10] P. Suri, R.P. Koseski, R.M. German, Mater. Sci. & Eng. A **402(1-2)**, 341 (2005).
[11] T. Tunberg, L. Nyborg, Powder Metall. **38(2)**, 120 (1995).
[12] R.M. Larsen, K.A. Thorson, Powder Metall. **37**, 61 (1994).

Received: 20 November 2014.